

# The Role of MmpL8 in Sulfatide Biogenesis and Virulence of *Mycobacterium tuberculosis*\*

Received for publication, January 12, 2004, and in revised form, March 3, 2004  
Published, JBC Papers in Press, March 4, 2004, DOI 10.1074/jbc.M400324200

Pilar Domenech‡, Michael B. Reed‡, Cynthia S. Dowd‡, Claudia Manca§, Gilla Kaplan§,  
and Clifton E. Barry III‡¶

From the ‡Tuberculosis Research Section, NIAID, National Institutes of Health, Rockville, Maryland 20852 and the §Public Health Research Institute, Newark, New Jersey 07103

To study the role of MmpL8-mediated lipid transport in sulfatide biogenesis, we insertionally inactivated the *mmpL8* gene in *Mycobacterium tuberculosis*. Characterization of this strain showed that the synthesis of mature sulfolipid SL-1 was interrupted and that a more polar sulfated molecule, termed SL-N, accumulated within the cell. Purification of SL-N and structural analysis identified this molecule as a family of 2,3-diacyl- $\alpha,\alpha'$ -D-trehalose-2'-sulfates. This structure suggests that transport and biogenesis of SL-1 are coupled and that the final step in sulfatide biosynthesis may be the extracellular esterification of two trehalose 6-positions with hydroxyphthioceranic acids. To assess the effect of the loss of this anionic surface lipid on virulence, we infected mice via aerosol with the MmpL8 mutant and found that, although initial replication rates and containment levels were identical, compared with the wild type, a significant attenuation of the MmpL8 mutant strain in time-to-death was observed. Early in infection, differential expression of cytokines and cytokine receptors revealed that the mutant strain less efficiently suppresses key indicators of a Th1-type immune response, suggesting an immunomodulatory role for sulfatides in the pathogenesis of tuberculosis.

Despite more than 100 years of research, tuberculosis continues to be a serious global health problem, and the bacterial factors that facilitate the intracellular survival and pathogenesis of this disease remain largely unknown. The unique mycobacterial envelope, rich in diverse biologically active lipids, not only provides a physical barrier from environmental factors and host damage but also presents multiple lipid species that can contribute directly to the pathology of mycobacterial disease (1–3).

The genome of *Mycobacterium tuberculosis* (MTb)<sup>1</sup> contains 12 genes that encode RND (resistance, nodulation, and cell

division) proteins designated MmpL (Mycobacterial membrane protein Large) (4). These proteins are characterized by the presence of 12 transmembrane domains and two extracytoplasmic loops and have been reported in the genomes of organisms from all major kingdoms of life. In Gram-negative bacteria, these proteins facilitate the transport of a large variety of drugs, heavy metals, aliphatic and aromatic solvents, bile salts, fatty acids, detergents, and dyes (5). In Gram-positive bacteria, an ActII-ORF3 mutant (a member of the same family of proteins) in *Streptomyces coelicolor* has been shown to be impaired for  $\gamma$ -actinorhodin production (6). In this case, both synthesis and transport of this complex polyketide were affected. The co-localization of some of the *mmpL* genes with genes involved in polyketide biosynthesis (*pks* genes) and genes involved in lipid metabolism (*papA* and *fadD*) suggests a similar role of these proteins in complex lipid transport in MTb (7, 8). Indeed, the MmpL7 protein has been shown to be involved in transport of phthiocerol dimycocerosate (PDIM) (9, 10).

One of the *mmpL* genes, *mmpL8*, is positioned 8 kbp downstream from the *pks2* gene. *Pks2* is involved in the synthesis of heptamethyl- and octamethyl-branched fatty acids (known as phthioceranic acids) present in the major sulfolipid of *M. tuberculosis*, SL-1 (11). Structural analysis of SL-1 was performed by Goren and co-workers (12–14), who identified it as 2-palmitoyl(stearoyl)-3-phthioceranol, 6,6'-bis(hydroxyphthioceranyl) trehalose 2'-sulfate. The low abundance of this molecule in cultured MTb, its unique presence in the pathogenic human tubercle bacillus, and numerous experimental studies over the past 40 years strongly suggest a role for SL-1 in virulence. Some studies have reported a significant correlation between virulence of different strains of *M. tuberculosis* in guinea pigs and the amount of SL-1 produced by these strains cultured *in vitro* (15, 16). Administration of *M. tuberculosis* sulfatides to cultured macrophages prevents phagosome-lysosome fusion (14), although this effect has been questioned since many anionic lipids could interact similarly with cationic sites on lysosomal hydrolases with resultant immobilization and/or inactivation of the enzymes (15). A role for SL-1 in blocking human macrophage and neutrophil activation by modulation of superoxide release and secretion of IL-1 $\beta$  and TNF- $\alpha$  also has been observed (17–21). In addition, *in vivo* and *in vitro* studies have shown that SL-1 and cord factor may synergize in terms of mouse toxicity and attack on mitochondrial structure and function (22). In contrast to these studies, two different groups (23, 24) have recently reported that *pks2* disruption and SL-1 deficiency do not significantly affect the replication, persistence, or pathogenicity of *M. tuberculosis* in mice, guinea pigs, or cultured macrophages.

In this study, we confirm and extend the recent observation by Converse *et al.* (23) that the synthesis of SL-1 is interrupted

\* This work was supported by National Institutes of Health, Public Health Service Grants AI-54361 and AI-22616 (to G. K.). The costs of publication of this article were defrayed in part by the payment of page charges. This article must therefore be hereby marked "advertisement" in accordance with 18 U.S.C. Section 1734 solely to indicate this fact.

¶ To whom correspondence should be addressed: Tuberculosis Research Section, Laboratory of Immunogenetics, 12441 Parklawn Dr., Rockville, MD 20852. Tel.: 301-435-7509; Fax: 301-402-0993; E-mail: cbarry@niaid.nih.gov.

<sup>1</sup> The abbreviations used are: MTb, *Mycobacterium tuberculosis*; RND, resistance, nodulation, and cell division; *mmpL*, mycobacterial membrane protein large; *pks*, polyketide synthase; PDIM, phthiocerol dimycocerosate; SL, sulfolipid; kbp, kilobase pair(s); TLC, thin layer chromatography; GC-MS, gas chromatography-mass spectrometry; EI-MS, electrospray ionization-mass spectrometry; MS/MS, tandem mass spectrometry; CFU, colony-forming unit(s).

in an MTb *mmpL8* mutant. This mutant accumulates a more polar molecule, termed SL-N, which is a likely precursor of SL-1. As a consequence, the cell surface charge appears to have been significantly altered. Purification and extensive analytical characterization of SL-N lead us to propose that, in contrast with the structure suggested by Converse *et al.* (23), this molecule is a family of 2,3-diacyl- $\alpha,\alpha'$ -D-trehalose-2'-sulfates. Finally, we show that although loss of the MmpL8 protein does not affect *in vivo* replication rate or bacterial numbers during chronic infection, it does attenuate virulence of MTb in murine survival studies.

#### EXPERIMENTAL PROCEDURES

**Bacterial Strains, Culture Conditions, and Plasmids**—The ElectroMAX DH5 $\alpha$  *Escherichia coli* strain (Invitrogen) used for cloning was grown in Luria-Bertani medium with hygromycin (200  $\mu$ g/ml) (Invitrogen) or gentamicin (Invitrogen) (5  $\mu$ g/ml) when indicated. MTb strains were grown in Middlebrook 7H9 broth (Difco) supplemented with ADC (NaCl, 8.1 g/liter; bovine albumin fraction V (Calbiochem), 50 g/liter; D-glucose, 20 g/liter), 0.02% glycerol, and 0.05% Tween 80 (Sigma) or on Middlebrook 7H11 agar (Difco) supplemented with OADC enrichment (as ADC but including also 0.6 ml/liter oleic acid (ICN Biochemicals) and 3.6 mM sodium hydroxide). Where indicated hygromycin (50  $\mu$ g/ml) or 2% sucrose was added (25). H37Rv (Pasteur) was used as the parental strain of the H37Rv *mmpL8::hyg* mutant and H37Rv (ATCC, Manassas, VA) for the generation of the *pkS2::hyg*.

**Nucleic Acid Techniques**—*E. coli* transformations, cloning, and PCR were based on standard conditions (26). Southern blotting and hybridization procedures were performed as described previously (27). Mycobacterial DNA was isolated using the protocol of Pelicic *et al.* (25). Transformation of MTb was carried out as described previously (28).

**Construction of the *mmpL8* and *pkS2* Disrupted Mutants**—Generation of the MTb disrupted mutants (*mmpL8::hyg* and *pkS2::hyg*) was accomplished by homologous recombination using the system developed by Pelicic *et al.* (25). A 2.1-kbp fragment containing the *mmpL8* gene (nucleotide positions 538–2686) was generated by PCR and cloned into the SpeI site of the vector pCDNA2.1 (Invitrogen). A 1.6-kbp fragment carrying the *hyg* gene was cloned into the *mmpL8* gene at the HpaI site (position 1656). Finally the 3.7-kbp fragment harboring the *mmpL8::hyg* gene was excised and cloned into the mycobacterial shuttle vector pPR27 (25). The *pkS2* mutant was produced by PCR amplification of a 2-kbp fragment containing the *pkS2* gene (positions 3302–5310). This fragment was cloned into the vector pCRBlunt (Invitrogen), and a 1.6-kbp fragment carrying the *hyg* gene was substituted for a 1-kbp internal NheI (position 4457)–BglII (position 4775) segment. The 2.6-kbp fragment containing the disrupted *pkS2* sequence and hygromycin resistance determinant was excised and cloned into the mycobacterial shuttle vector pPR27 (25). Transformations were plated on 7H11 with 50  $\mu$ g/ml hygromycin at 32 °C for 5 weeks. The resulting colonies were grown at 32 °C in 10 ml of 7H9 containing 50  $\mu$ g/ml hygromycin and subsequently were plated on 7H11 with 50  $\mu$ g/ml hygromycin and 2% sucrose at 39 °C. DNA from Hyg<sup>R</sup>, Suc<sup>R</sup>, and T<sup>R</sup> (hygromycin-, sucrose-, and temperature-resistant) colonies was digested with XhoI, transferred to Hybond-N nylon membrane (Amersham Biosciences) by Southern blot, and hybridized with a 2.1-kbp fragment probe of the *mmpL8* gene of MTb H37Rv Pasteur. The *pkS2::hyg* deletion-replacement was confirmed through Southern analysis of EcoRI- or EcoRV-restricted DNA that was hybridized with both the 2-kbp *pkS2* fragment generated by PCR (see above) and the 1-kbp fragment released prior to insertion of the hygromycin cassette.

**Lipid Analysis and Sulfolipid Purification**—100-ml cultures of the different MTb strains (wild type, *mmpL8::hyg*, and *pkS2::hyg* mutants) were grown to an OD<sub>650</sub> of 0.3. Metabolic labeling of the methyl-branched fatty acids was achieved by incubating these cultures in the presence of 1  $\mu$ Ci/ml sodium [1-<sup>14</sup>C]propionate (American Radiolabeled Chemicals, specific activity  $\approx$  56 mCi/mmol) for 24 h prior to lipid extraction. Similarly, sulfated lipids were labeled by adding 3.3  $\mu$ Ci/ml [<sup>35</sup>S]Na<sub>2</sub>SO<sub>4</sub> (Amersham Biosciences, specific activity  $\approx$  100 mCi/mmol) and incubated for 96 h. Mycobacteria were harvested from the media by centrifugation (750 g/15 min), and prior to lipid extraction the culture supernatants were sterilized by filtration through a 0.2- $\mu$ m-pore size membrane. Bacteria-associated lipids were extracted by two different methods. Bacteria-associated total lipids were extracted using the Folch method (29), which includes two extractions with chloroform:methanol (2:1) and three washes with chloroform, methanol, and 0.58% NaCl in water at ratios 3:48:47. Alternatively, separation of bacteria-

associated apolar and polar lipids was accomplished by two petroleum ether extractions (apolar) prior to chloroform:methanol extraction, following the procedures described by Slayden and Barry (30). Apolar lipids present in the culture supernatant were extracted with 2 volumes of petroleum ether. Polar lipids in the supernatant were extracted as described elsewhere (31). Thin layer chromatography (TLC) was performed using 250- $\mu$ m silica gel 60 plates (EM SCIENCE) with chloroform:methanol:H<sub>2</sub>O (65:25:4) as the developing solvent. TLC plates were visualized using a Storm 860 PhosphorImager (Amersham Biosciences).

For purification of SL-1 and SL-N, 4-liter cultures of H37Rv and *mmpL8::hyg* were labeled with 1 mCi of [<sup>35</sup>S]Na<sub>2</sub>SO<sub>4</sub> (Amersham Biosciences, 100 mCi/mmol) as is indicated above. Bacteria-associated lipids (apolar for SL-1, polar for SL-N, prepared as above) were passed over a silica gel 50 column and eluted with 9:1 chloroform:methanol (3 volumes), 5:1 chloroform:methanol (3 volumes), and 1:1 chloroform:methanol (6 volumes). Fractions containing sulfolipids were identified by TLC and autoradiography and were then pooled and dried. Next, the pooled fractions were applied to an anion exchange column (PS-DVB DEAE, 10 mm  $\times$  100 mm, 8- $\mu$ m beads, Vydac) on a Waters 2690 HPLC. The column was activated prior to injection of the sample by equilibrating with chloroform:methanol:acetic acid (800:200:0.6) at a flow rate of 2 ml/min. Elution of the lipids was done using a 0–35% gradient over 40 min with chloroform:methanol:triethylamine (800:200:1.39) as the eluting solvent. 2-ml fractions were collected and analyzed by liquid scintillation counting and TLC. Purity of samples was assessed by staining TLC plates with 5% phosphomolybdic acid (Sigma) and charring.

**Neutral Red Assay**—Chemical staining of H37Rv and the *mmpL8::hyg* strain was carried out following the protocol described by Soto *et al.* (32).

**GC-MS of Fatty Acid Methyl Esters**—Fatty acid methyl esters from purified SL-1 and SL-N were prepared following the protocol described previously (30). GC-MS was carried out on a Hewlett Packard 5890 instrument operated in splitless mode using an HP-5MS column (30 m  $\times$  0.25 mm  $\times$  0.25  $\mu$ m). The injection port temperature was 310 °C, and the column temperature was ramped from 180 to 310 °C at 10 °C/min followed by an additional 15 min at 310 °C with 8 p.s.i. helium.

**Mass Spectrometry**—Mass spectral analyses were performed at the Yale Cancer Center Mass Spectrometry Resource and the W. M. Keck Foundation Biotechnology Resource Laboratory. For both electrospray ionization-mass spectrometry (EI-MS) and tandem mass spectrometry (MS/MS), purified SL-N was dissolved in chloroform and then diluted with methanol, 1% ammonium hydroxide (for negative ion analysis) or methanol, 1% formic acid (for positive ion analysis) to a useable concentration. The samples were analyzed on a Q-ToF1 (Waters/Micro-mass) mass spectrometer using the nanospray technique for both positive and negative modes. For the MS/MS spectra, the collision cell was pressurized with argon, and the collision energy was adjusted to give the optimal spectrum, which was –4 electron volts for positive ion spectra and –70 electron volts for negative ion spectra. The spectra were calibrated using sodium iodide in either the positive or negative ion mode.

**Proton and COSY NMR Spectra**—The <sup>1</sup>H (one-dimensional) and COSY spectra of <sup>35</sup>S-labeled SL-N were obtained on a Varian VXR-500S NMR spectrometer at 30 °C in CDCl<sub>3</sub>:CD<sub>3</sub>OD (2:1).

**Mouse Experiments**—Prior to infection, well dispersed liquid cultures were adjusted to an OD<sub>650 nm</sub> of 0.5 and stored at –70 °C as 20% glycerol stocks. Inocula were prepared by diluting these stocks to 4  $\times$  10<sup>6</sup> colony-forming units (CFU)/ml in PBS/Tween 80 (0.05%). Eight-week-old C57Bl/6 or B6D2/F1 mice (Taconic) were infected using a BioAerosol nebulizing generator (CH Technologies Inc., Westwood, NJ) for 10 min. Bacterial numbers were enumerated at 1, 14, 49, 63, 98, 182, and 205 days post-infection (4 mice/time point) by homogenizing the lungs and spleens of infected mice in 1 ml of 7H9 medium and plating 10-fold serial dilutions on 7H11 medium. An additional 12 mice/group were used in survival studies. Survival fractions were calculated using the Kaplan-Meier method (33), and the log-rank test was used to determine statistical significance of observed survival differences (GraphPad Prism version 3.0; GraphPad Software, San Diego, CA).

**Cytokine Expression Studies**—At 14 days post-infection, lungs of euthanized mice (4 mice/group) were removed and immediately snap-frozen on dry ice/ethanol. Tissues were homogenized in 3 ml of RNazolB (Cinna/BiotecX, Houston, TX) using a tissue Polytron homogenizer. RNA was extracted according to the manufacturer's instructions, and 5  $\mu$ g of RNA from each sample was reverse transcribed into cDNA with Moloney murine leukemia virus reverse transcriptase (Ambion). Biotinylated cDNA probes were hybridized to cytokine-chemokine cDNAs spotted on GEArray membranes according to the manufacturer's direc-

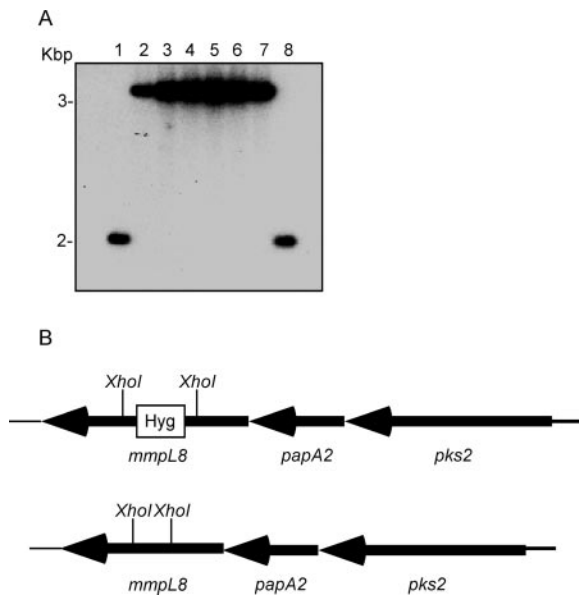


FIG. 1. Construction of the *M. tuberculosis* *mmpL8::hyg* mutant. A, Southern blot analysis of MTb recombinants. DNA from six colonies that were Hyg<sup>R</sup>, Suc<sup>R</sup>, and T<sup>R</sup> (lanes 2–7) and from MTb H37Rv (lanes 1 and 8) were digested with XhoI and hybridized with a 2-kbp fragment of the *mmpL8* gene of MTb H37Rv. The expected sizes were 2.1 kbp for the wild-type fragment and 3.7 kbp for legitimate double recombinants. B, genetic organization of the *mmpL8* locus in H37Rv and the *mmpL8::hyg* mutant.

tions (SuperArray, Bethesda, MD). Arrays were developed with CDP-Star chemiluminescence substrate and recorded with x-ray film. The ScanAnalyze 2 program was used for image analysis, and the GEArray-Analyzer was used to process the raw data. Gene expression was normalized to the signal derived from  $\beta$ -actin. 2-fold difference in mRNA expression between strains was considered significant.

## RESULTS

**Disruption of the MTb *mmpL8* Gene Interrupts SL-1 Biosynthesis**—Disruption of the *mmpL8* gene in MTb H37Rv was accomplished by insertion of a hygromycin resistance cassette within the coding sequence of a cloned copy of this gene followed by homologous recombination of the inactivated allele onto the chromosome of MTb using a plasmid based on the pPR27 vector (temperature-sensitive mycobacterial origin of replication and *sacB* negative selection marker) (25). Fig. 1A shows the results of Southern blot analysis of chromosomal DNA from six clones (lanes 2–7) obtained from this procedure compared with DNA from the H37Rv wild-type parent (lanes 1 and 8). In each clone the presence of a 3.7-kbp fragment hybridizing with an *mmpL8* probe that recognizes a 2.1-kbp fragment on the wild-type chromosome suggests that all six have the expected 1.6-kbp insertion of the hygromycin resistance cassette. One of these mutants was selected for further analysis.

Because of the chromosomal co-localization of *mmpL8* and *pks2* (Fig. 1B), we examined lipid extracts from the *mmpL8::hyg* mutant following metabolic labeling of the methyl-branched fatty acids of MTb H37Rv, MTb H37Rv *mmpL8::hyg*, and an MTb H37Rv *pks2::hyg* mutant with [1-<sup>14</sup>C]propionic acid. Bacteria-associated “apolar” (petroleum ether-extractable) and “polar” (chloroform:methanol-extractable) lipids were obtained from these strains and analyzed by TLC (Fig. 2A, lanes 1–8). SL-1, with an  $R_F$  of 0.92, was mainly extracted in the apolar fraction, suggesting localization within the peripheral region of the cell wall. SL-1 was present in both H37Rv wild-type strains tested (the type strain from the American Type Tissue Collection and the sequenced strain from the Institut Pasteur) (Fig. 2A, lanes 1, 3, 5, and 7). As expected

SL-1 was not produced by an MTb *pks2* mutant (Fig. 2A, lanes 4 and 8), but surprisingly the MTb *mmpL8::hyg* mutant also failed to produce mature SL-1 (lanes 2 and 6). This mutant instead accumulated a more polar metabolite ( $R_F$  0.5) that incorporated propionate and appeared in the polar fraction (Fig. 2A, lane 6).

To establish whether this metabolite contained sulfate we labeled cells by growing them in the presence of [<sup>35</sup>S]Na<sub>2</sub>SO<sub>4</sub> (Fig. 2A, lanes 9–12). In the wild-type strain the majority of the [<sup>35</sup>S]Na<sub>2</sub>SO<sub>4</sub> was incorporated into SL-1 (Fig. 2A, lanes 9 and 11), confirming that this was the most abundant sulfolipid produced in MTb. In contrast, the *mmpL8* mutant incorporated [<sup>35</sup>S]Na<sub>2</sub>SO<sub>4</sub> into a molecule that co-migrated by TLC with the propionate-labeled metabolite ( $R_F$  0.5) (Fig. 2A, lane 10). These results suggest that inactivation of the *mmpL8* gene of MTb interrupted the normal biosynthesis of SL-1 and led to the accumulation of a more polar molecule, designated SL-N, that contained both sulfate and methyl-branched fatty acids.

**SL-N Is Localized Inside the Cell Envelope**—We compared lipids associated with bacterial cells (Fig. 2B, lanes 1–4) with those found in the culture supernatant (Fig. 2B, lanes 5–8) for wild-type and *mmpL8::hyg* mutant strains. SL-1 was present in both the apolar and polar lipid extracts of wild-type culture supernatant (Fig. 2B, lanes 5 and 7), whereas SL-N was not found in the supernatant from the *mmpL8* mutant (lanes 6 and 8). While some SL-1 was also found in association with the bacterial cells, SL-N was found exclusively in association with the bacterial cells. This result suggests that SL-1 normally occupies a peripheral location within the mycobacterial envelope and can be shed into the culture supernatant, whereas SL-N apparently occupies a more integral location and may be exclusively retained within the cytosol.

In an attempt to address whether SL-N was peripherally associated with the cell membrane but was not efficiently shed into the medium, we examined the neutral red binding ability of the *mmpL8::hyg* mutant. The neutral red assay has been used extensively to distinguish between avirulent and virulent strains of MTb because of its specificity for labeling cells producing SL-1 (15, 32, 34, 35). The capacity to bind this molecule has been interpreted as indicating a surface-accessible location of the sulfatides, whose strongly acidic sulfate interacts ionically with the cationic dye (36). We performed the neutral red assay following the method described by Soto *et al.* (32). As shown in Fig. 2C, the wild-type strain gave the expected red coloration, while the *mmpL8::hyg* mutant showed only a dim yellow color, supporting the conclusion that SL-N is not localized at the cell surface. Together, these experiments suggest that SL-N is not secreted to the mycobacterial cell surface and that the absence of this molecule from the cell surface results in a significant alteration in overall charge at the region of the cell envelope most likely to interact directly with the host during infection.

**Purification and Acyl Group Composition of SL-N**—To analyze the structure of SL-N, we extracted and purified this molecule and SL-1 from 4 liters of <sup>35</sup>S-labeled *mmpL8::hyg* mutant and wild-type strains, respectively. These two molecules were purified by a combination of silica gel chromatography and anion-exchange (DEAE) high pressure liquid chromatography. The yield of purified material was 0.05 mg of SL-1/g of MTb H37Rv cells and 0.11 mg of SL-N/g of MTb *mmpL8::hyg* mutant cells.

Initially, we attempted to define the acyl group composition of these two molecules by preparation of methyl esters of fatty acids resulting from saponification of SL-1 and SL-N. Analysis of the resulting fatty acid methyl esters by GC-MS showed chromatograms for SL-1 and SL-N that were remarkably sim-

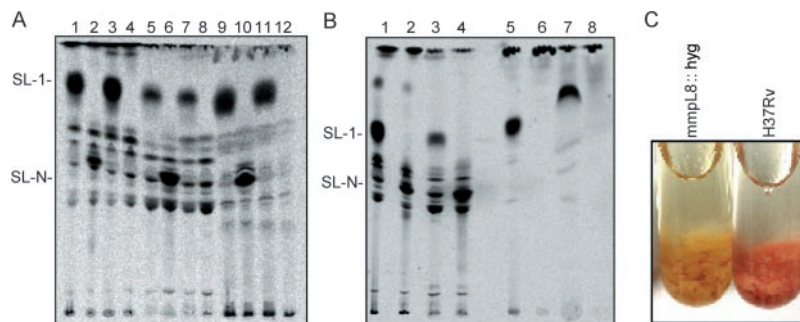


FIG. 2. Disruption of the *M. tuberculosis* *mmpL8* gene interrupts SL-1 biosynthesis and results in accumulation of SL-N. A, autoradiogram of a TLC of [1-<sup>14</sup>C]propionic acid-labeled (lanes 1–8) and [<sup>35</sup>S]Na<sub>2</sub>SO<sub>4</sub>-labeled (lanes 9–12) lipids developed in chloroform:methanol:water (65:25:4). Lanes 1–4 are bacteria-associated “apolar lipids” (extracted with petroleum ether). Lanes 5–8 are bacteria-associated “polar lipids” (extracted with chloroform:methanol (2:1) after the petroleum ether extraction), and lanes 9–12 are bacteria-associated total lipids (total lipids extracted with chloroform:methanol (2:1) following the Folch method). Lipids are from H37Rv (Pasteur strain; lanes 1, 5, and 9), *mmpL8::hyg* mutant (lanes 2, 6, and 10), H37Rv (ATCC 27294; lanes 3, 7, and 11), and *pks2::hyg* mutant (lanes 4, 8, and 12). B, autoradiogram of a TLC of [1-<sup>14</sup>C]propionic acid-labeled bacteria-associated lipids (lanes 1–4) and lipids extracted from the culture supernatants (lanes 5–8). Lanes 1 and 5, apolar lipids from H37Rv (Pasteur); lanes 2 and 6, apolar lipids from *mmpL8::hyg* mutant; lanes 3 and 7, polar lipids from H37Rv (Pasteur); lanes 4 and 8, polar lipids from *mmpL8::hyg* mutant. The solvent is chloroform:methanol:H<sub>2</sub>O (65:25:4). C, neutral red assay of H37Rv (Pasteur) and *mmpL8::hyg* (*mmpL8* KO).

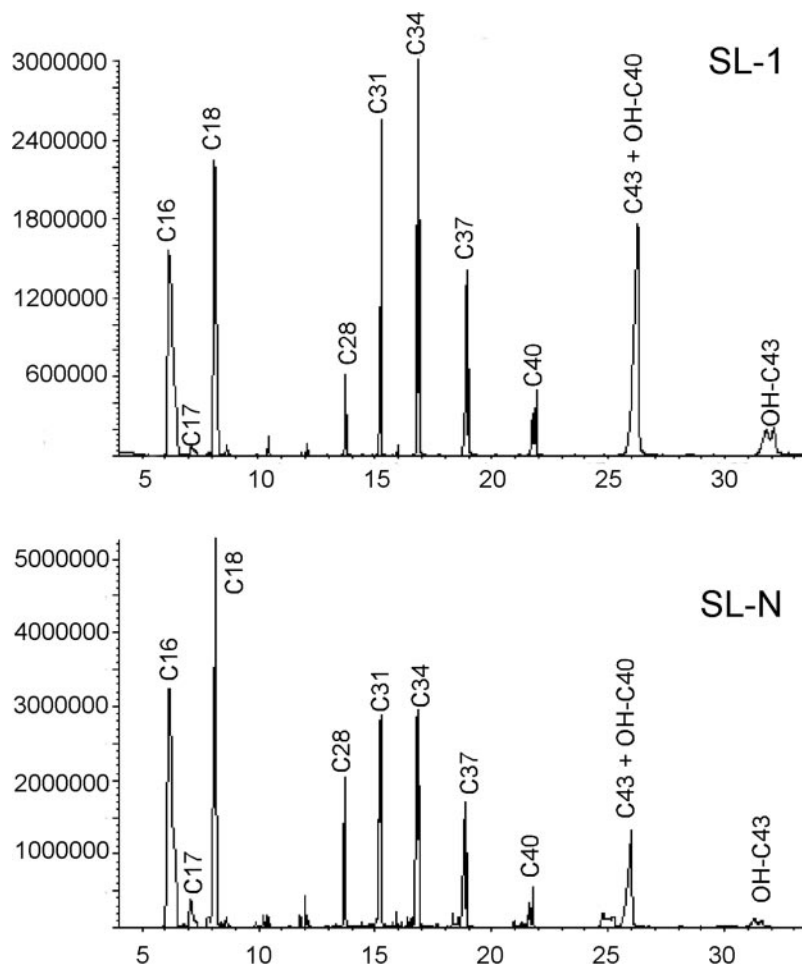


FIG. 3. Characterization of the fatty acid methyl esters present in SL-N. GC-MS of fatty acid methyl esters obtained from purified SL-1 and SL-N molecules was performed. Representative chromatograms from each molecule after saponification and methylation of component lipids are shown. These analyses were performed a minimum of three independent times with similar results. Peaks were identified by comparison with synthetic standards and/or by comparison of the mass spectra and predicted fragmentation patterns with reference libraries.

ilar (Fig. 3). Both chromatograms showed major peaks with retention times of 6.14, 7.09, 8.17, 13.71, 15.24, 16.83, 18.80, 21.78, 26.00, and 32.12 min. The molecular ions of the first three peaks were *m/z* 270, 284, and 298, respectively, corresponding to C<sub>16</sub> (palmitate), C<sub>17</sub> (14-methylhexadecanoic acid), and C<sub>18</sub> (stearate) fatty acids. The remaining peaks all contained characteristic fragment ions of  $\alpha$ -methyl-branched fatty acids at *m/z* 88 and 101. The presence of these peaks in both spectra confirmed that SL-N, like SL-1, contained  $\alpha$ -methyl-branched fatty acids consistent with the observed labeling by

[1-<sup>14</sup>C]propionate. The molecular ions found in the peaks eluting between 13 and 22 min were at *m/z* 438, 480, 522, 564, and 606, respectively (data not shown). These molecular ions are identical to those described by Goren and co-workers (13) in the original description of the phthioceranyl acyl substituents of SL-1 corresponding to the series of total carbon length C<sub>28</sub>, C<sub>31</sub>, C<sub>34</sub>, C<sub>37</sub>, and C<sub>40</sub> (palmitate extended by 4–8 propionates). The broad peak at 26 min suggested that there could be more than one molecule eluting at this retention time. The major high molecular weight ion observed for this peak (383 *m/z*) corre-

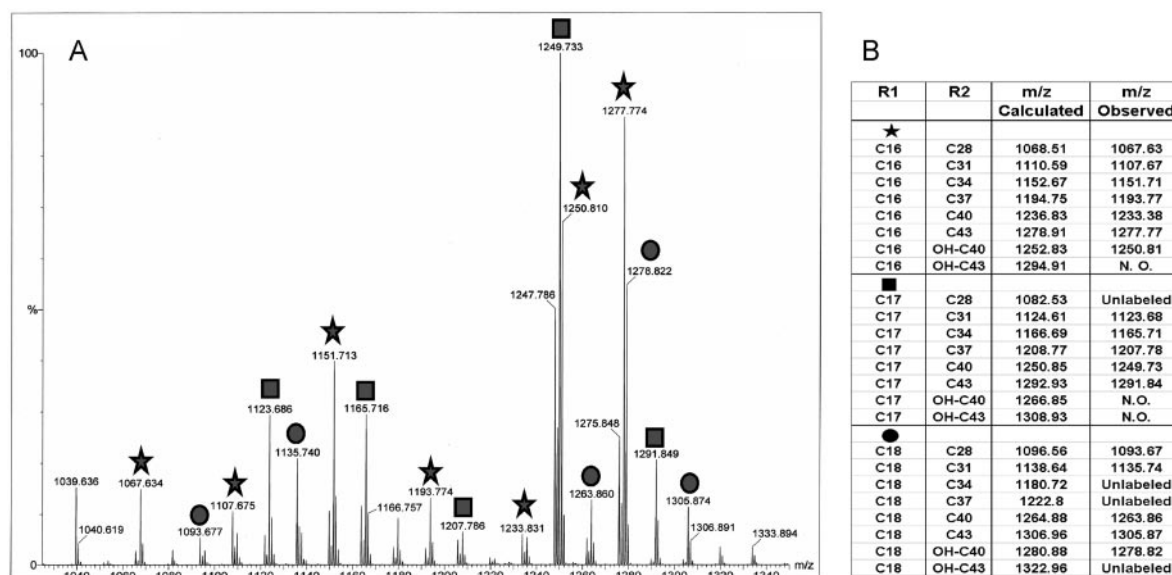


FIG. 4. **Electrospray ionization-mass spectrometry and composite lipids of SL-N species in the *mmpL8::hyg* mutant.** A, negative mode EI-MS spectrum of purified SL-N from *mmpL8::hyg* mutant. B, calculated and observed  $m/z$  of the different molecules comprising SL-N. The three series of molecules are grouped by their shorter acyl chain that presumably occupies the 2-position of trehalose (R1 = C<sub>16</sub>; ★; C<sub>17</sub>; ■; and C<sub>18</sub>, ●). N.O., not observed.

sponded to the methyl-branched portion of a C<sub>40</sub> hydroxyphthioceranic ester (M-239), as was described previously (13). Thus this fragment was likely composed of eight propionic acid units. An associated peak at  $m/z$  411 ((M-240) + 29) was also observed, supporting the structure of this fatty acid. The molecular ion, however, observed in the spectrum ( $m/z$  649) did not correspond to C<sub>40</sub> hydroxyphthioceranic ester but to C<sub>43</sub> phthioceranic ester (a palmitic moiety condensed with nine propionic acids). In fact, this molecular ion was most visible at the later eluting portion of the peak, not at the apex. Therefore, we conclude that this peak corresponded to a mixture of the C<sub>40</sub> hydroxyphthioceranic methyl ester and the C<sub>43</sub> phthioceranic methyl ester. The peak at 32.12 min showed a mass at  $m/z$  425 (M-239), identical to that observed for the C<sub>43</sub> hydroxyphthioceranic methyl ester, as well as an associated peak at  $m/z$  453 (nine propionic acid moieties plus a hydroxymethylene unit) (13). No molecular ion was detected in this peak.

The presence of the same species of fatty acids in both SL-1 and SL-N was surprising given the differences in polarity of these molecules in TLC. In addition, the identification of non-hydroxylated phthioceranic acid as one of the fatty acids esterified on the trehalose is in contrast to the reported lack of this molecule in the study by Converse *et al.* (23). There did appear to be a quantitative difference in the total amounts of hydroxyphthioceranic and phthioceranic compared with the amounts of short-chain acyl constituents seen, but because we observed significant variability in the relative volatilization and detection efficiencies of these molecules, we did not attempt to quantitate these by integration of the total ion current.

**SL-N Is a Mixture of Sulfated Diacyltrehaloses**—Analysis of SL-N by EI-MS in negative mode is shown in Fig. 4A. While the molecular mass of the various species that comprise SL-1 lies between  $m/z$  2400 and 2600 (12, 37), the major molecular ions observed in the SL-N EI-MS spectrum were found between  $m/z$  1039.64 and 1333.89. This difference in mass (more than 1000 units between SL-1 and SL-N) suggests the presence of only two fatty acids in SL-N as compared with four in SL-1. Considering the GC-MS studies that demonstrated the presence of straight-chain, methyl-branched, and hydroxylated, methyl-branched fatty acids in SL-N, the ions in the EI-MS can be fully

interpreted as a mixture of sulfated diacyltrehaloses where the acyl groups of the individual species include one shorter chain (C<sub>16</sub>–C<sub>18</sub>) and one longer chain (C<sub>28</sub>–C<sub>43</sub>) (saturated and hydroxylated) fatty acid (Fig. 4B). The straight-chain fatty acid (R1) can be C<sub>16</sub>, C<sub>17</sub>, or C<sub>18</sub>, while the phthioceranic acid (R2) may (C<sub>40</sub> or C<sub>43</sub>) or may not (C<sub>28</sub>, C<sub>31</sub>, C<sub>34</sub>, C<sub>37</sub>, C<sub>40</sub>, or C<sub>43</sub>) be hydroxylated. Calculated and observed masses of the three proposed series (C<sub>16</sub>, C<sub>17</sub>, and C<sub>18</sub>) are indicated in the table in Fig. 4B.

In addition to the molecular ions observed in the primary EI-MS, MS/MS indicated the presence of an unsubstituted sulfolipid in each peak observed (259/241 ion pair in negative mode, data not shown). This result suggests that both acyl groups are esterified to the non-sulfated glucose ring of trehalose and conflicts with the structure assigned previously by Converse *et al.* (23) of SL<sub>1278</sub>, the molecule accumulated within their *mmpL8* mutant.

**Acylation of SL-N Is at C-2 and C-3 Positions of the Trehalose Ring**—The acylated positions of the trehalose were confirmed through COSY NMR analysis of purified SL-N (Fig. 5A). The anomeric protons appear at  $\delta$ 5.06 and 5.25 ppm. The doublet at  $\delta$ 5.06 ppm ( $J$  = 3.8 Hz) formed a cross-peak with an upfield doublet of doublets ( $\delta$ 3.48 ppm,  $J$  = 9.8, 3.7 Hz), which corresponds to the proton adjacent to the 2'-sulfate, and was, therefore, assigned as the H-1' anomeric proton, consistent with previous descriptions (38). The H-2' signal was observed to be coupled to the doublet at  $\delta$ 3.74 ppm ( $J$  = 9.3 Hz), which was therefore assigned as the H-3' proton. The cross-peaks from the H-3' signal revealed coupling to a multiplet at  $\delta$ 3.36–3.40 ppm (H-4'), the multiplet at  $\delta$ 3.51–3.55 ppm (H-5'), the multiplet at  $\delta$ 3.63–3.70 ppm (H-6'a), and the doublet of doublets at  $\delta$ 3.80 ppm (H-6'b,  $J$  = 12.1, 2.5 Hz). The multiplet at  $\delta$ 3.63–3.70 ppm and the signals between  $\delta$ 3.47 and 3.55 ppm integrated for three protons each, consistent with these assignments. The doublet at  $\delta$ 5.25 ppm ( $J$  = 3.5 Hz) is the H-1 anomeric proton and showed a cross-peak with the doublet of doublets at  $\delta$ 4.83 ppm (H-2,  $J$  = 10.3, 3.6 Hz), which in turn formed a cross-peak with the doublet of doublets at  $\delta$ 5.39 ppm (H-3,  $J$  = 10.2, 9.3 Hz). From H-3, cross-peaks were found to the multiplet at  $\delta$ 3.50–3.51 ppm (H-4), the multiplet at  $\delta$ 3.89–3.93 ppm (H-5), and two protons within the multiplet at  $\delta$ 3.63–3.70 ppm (H-6a

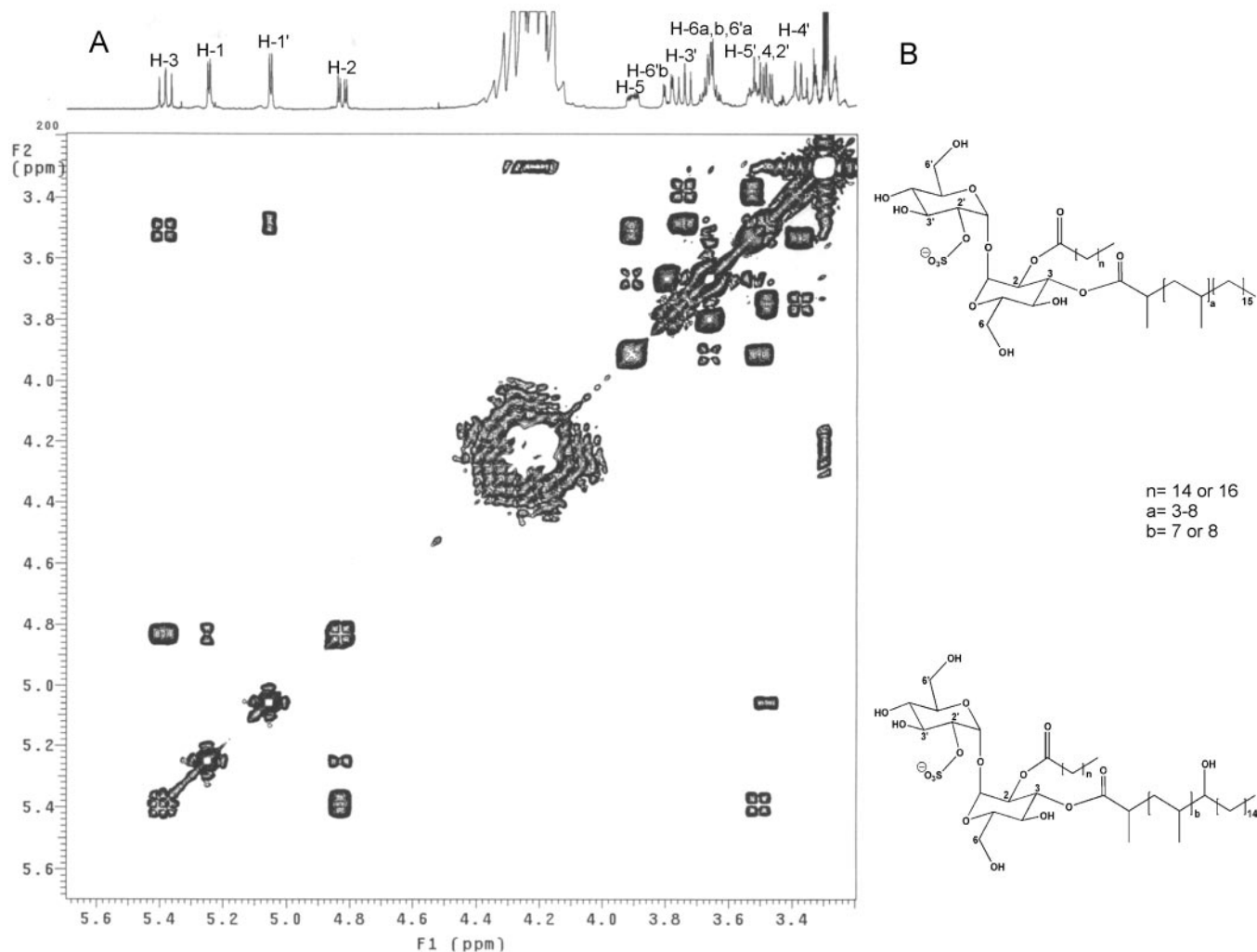


FIG. 5. **Determination of the location of the acyl groups attached to SL-N.** A, COSY NMR of SL-N. The region from  $\delta$ 3.2 to 5.7 ppm corresponding to the chemical shifts of protons directly attached to trehalose is shown. B, SL-N structure. Two homologous series of molecules with either phthioceratanate (*top*) or hydroxyphthioceratanate (*bottom*) at the 3-position are shown.

and H-6b). Supporting this assignment, Baer (39) reported the separation of the H-6'a and H-6'b protons in an unsubstituted ring, while the chemical shifts of these protons in an acylated ring overlapped (39). Integration of the H-1, H-1', H-2, and H-3 protons was equivalent, indicating that each represented a single proton. The downfield chemical shifts of the H-2 and H-3 protons, relative to all other non-anomeric protons, indicated that these sites are acylated. These results demonstrate that, as suggested by the observation of only unsubstituted sulfolipid in the MS/MS spectra, acylation of SL-N is exclusively at positions 2 and 3 of the non-sulfated glucose of the trehalose ring system (Fig. 5B).

**Lack of MmpL8 Alters the Virulence Properties of MTb**—The role of MmpL8 in the virulence of MTb was studied using a low dose aerogenic murine model of infection. Two different mouse strains (C57Bl/6 and B6D2/F1) were infected with  $\sim$ 100 CFU of either the *mmpL8::hyg* mutant or the parental H37Rv strain. The average initial number of bacteria implanted in the first experiment using C57Bl/6 mice was 62 CFU/lung for H37Rv and 78 CFU/lung for the *mmpL8::hyg* mutant. In the second experiment with B6D2/F1 mice, the initial CFU were found to be 169 and 160, respectively. In both cases the growth kinetics of the two strains were identical throughout the infection, indicating that loss of MmpL8 did not affect initial bacterial replication or containment of this replication in the lungs and spleens of these animals (Fig. 6, A, B, and D). The 12 mice

remaining in each group were observed until they died in survival experiments that extended over a period of 370 and 220 days, respectively. The first experiment demonstrated that although the *mmpL8* mutant was not impaired for growth in C57Bl/6 mice, the mice infected with this strain survived longer (mean = 328 days) than those infected with the parental H37Rv strain (mean = 265 days,  $p$  value = 0.0006, Fig. 6C). This result was confirmed in the second experiment where wild-type infected mice showed a mean survival time of 154 days. Among mice infected with the *mmpL8::hyg* mutant, only three mice had died 220 days post-infection when the experiment was terminated (Fig. 6E). These results indicate that although MmpL8 is not required for *in vivo* growth of MTb, the lack of this protein significantly alters the final outcome of the infection.

Long term survival in such experiments has been correlated previously with granuloma structure, which may be influenced by the initial cytokine response (2, 3). We therefore performed a preliminary evaluation of the level of expression of indicator cytokine genes in mice early in infection. RNA was extracted from lungs of mice infected for 14 days, and cDNA was hybridized to cytokine-chemokine-specific GEArray membranes. Fig. 6F shows the ratio of genes that are overexpressed in mice infected with the parental strain at a level greater than 5 $\times$  the level observed in those infected with the *mmpL8* mutant. The cytokines whose expression was most highly affected included

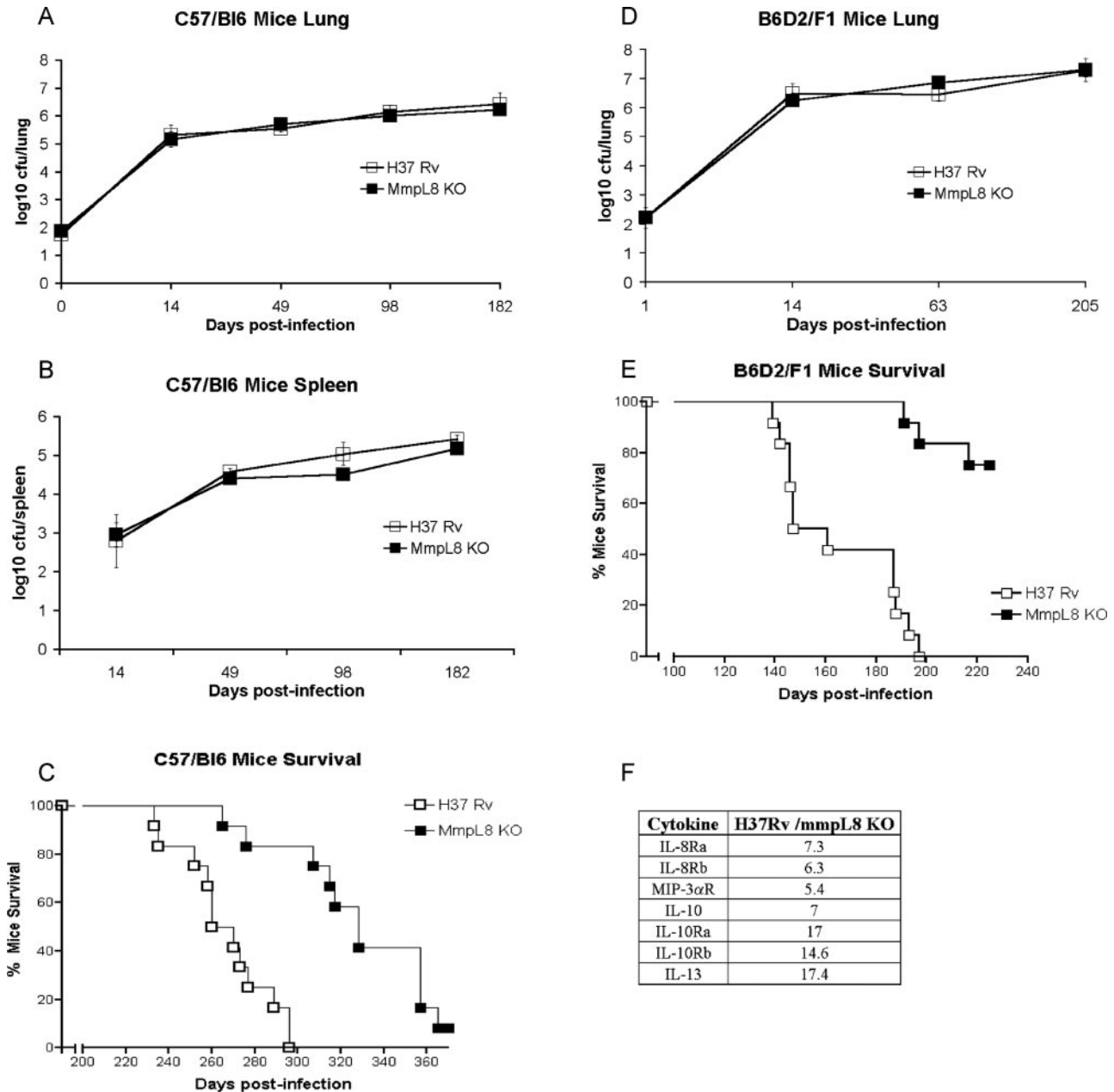


FIG. 6. **MmpL8 contributes to virulence of MTb in mice.** C57/Bl6 (A, B, and C) or B6D2/F1 (D, E, and F) mice were infected aerogenically either with the *mmpL8::hyg* mutant (MmpL8 KO) (filled squares) or the parental strain H37Rv (open squares). Bacterial numbers were monitored at the indicated times post-infection by harvesting lung (A and D) and spleen (B) of infected mice. Results are expressed as an average of log<sub>10</sub> CFU/lung (or log<sub>10</sub> CFU/spleen) along with the standard deviation obtained from replicate platings. C and E, mice were evaluated in a time-to-death experiment for both the *mmpL8::hyg* mutant (MmpL8 KO) (filled squares) and the parental strain H37Rv (open squares). Analysis of this data was done using the Kaplan-Meier method, and a log-rank test was used to determine statistical significance of observed survival differences (GraphPad Prism version 3.0; GraphPad Software). F, differential cytokine and cytokine receptor expression in B6D2/F1 mice infected with H37Rv or *mmpL8::hyg* mutant (MmpL8 KO) at 14 days post-infection. The results shown are the ratio of expression in wild type versus *mmpL8::hyg* mutant.

IL-10 and IL-13, Th2 lymphocyte-derived cytokines that have potent anti-inflammatory properties.

#### DISCUSSION

In this study we show that the synthesis of the major sulfatide of *M. tuberculosis*, SL-1, is interrupted in an *mmpL8* mutant strain indicating that this membrane protein is involved in the transport of this molecule or its precursor. This strain accumulates a sulfolipid of lower molecular weight and higher polarity, SL-N, indicating that transport and biosynthesis of SL-1 are tightly coupled. Together with the inability of the *mmpL8::hyg* mutant to fix the cationic dye neutral red, the

absence of this molecule in the culture supernatant and in the apolar extractable lipids of the mycobacterial envelope suggests that it accumulates within the cell envelope.

We have purified SL-N and established its structure in comparison with SL-1 using GC-MS, EI-MS, and COSY NMR. The results of these studies establish that SL-N is a 2,3-diacetyl- $\alpha,\alpha'$ -D-trehalose-2'-sulfate containing both short-chain acyl components and multimethyl-branched long-chain derivatives of either phthioceranic or hydroxyphthioceranic acid. While this study was in progress, others authors (23) also reported the accumulation of a novel sulfolipid in an independently generated mutant in the *mmpL8* gene in MTb. These authors pur-

tially purified this novel species by preparative TLC from cultures labeled with stable isotopes of sulfur and used Fourier transform ion cyclotron resonance mass spectrometry for characterization. They observed a series of isoforms ranging in size from  $m/z$  1270 to 1450 and further characterized one of these occurring at  $m/z$  1278 (designated SL<sub>1278</sub>) by exact mass measurements as a sulfated diacyl trehalose. By precedent with the established structure of SL-1, they assumed that the short-chain acyl group was located at the 2-position of the non-sulfated glucose ring of the trehalose. They stipulated that they could not assign the position of the predicted hydroxyphthioceranate residue they had proposed but suggested that it was esterified to the 6'-position of the sulfated trehalose. They therefore concluded that this molecule was likely to be 2,6'-diacyl- $\alpha,\alpha'$ -D-trehalose-2'-sulfate with a palmitate group in the 2-position and a C<sub>42</sub>-hydroxyphthioceranic acid at position 6'. No experimental evidence has been shown so far confirming the presence of this C<sub>42</sub>-hydroxyphthioceranic acid in SL-1. In contrast our more complete analysis of the structures of this family of molecules suggests that the sulfated diacyl trehalose species observed at 1278 is in fact 2-palmitoyl-3-(C<sub>43</sub>)-phthioceranyl- $\alpha,\alpha'$ -D-trehalose-2'-sulfate.

Perhaps more importantly from our data the major species observed are of slightly lower molecular weight and contain both phthioceranate and hydroxyphthioceranate moieties. Further, the COSY NMR demonstrates convincingly that the substitution pattern of the two acyl groups is 2,3 rather than 2,6'. However, like Converse *et al.* (23), we cannot conclusively state which acyl group occupies each position and again assign the shorter chain component to the 2-position based upon precedent (40). Although in SL-1 the major substituents reported at the 3-position are phthioceranic acids with hydroxyphthioceranic acids occurring at the two 6-positions, in some sulfatides these positions were interchanged (40) indicating that the acyltransferase that catalyzes the reaction at the 3-position can utilize either phthioceranic acids or hydroxyphthioceranic acids. The presence of hydroxyphthioceranic acids at the 3-position of SL-N supports this idea. It might also be reasonably anticipated that in the *mmpL8::hyg* mutant, unused hydroxyphthioceranic acids would accumulate and as a consequence appear overrepresented in SL-N as we observe.

Our proposed SL-N structure suggests that acylation at the 2- and 3-position of the trehalose-2'-sulfate occurs in the cytoplasm generating a 2,3-diacyl sulfotrehalose, SL-N, that is then transported through the mycobacterial membrane by the MmpL8 protein. The final addition of the two remaining hydroxyphthioceranic acids at positions 6 and 6' would then be an extracytoplasmic process. The acyltransferase involved in this step has not been identified yet, although a candidate could be the secreted protein Ag85C, which has been shown to be involved in the transfer of fatty acids to the 6- and 6'-positions of trehalose (41).

Besides the essential role of MmpL8 in synthesis of SL-1, we have also shown that mature sulfatides may play an important but subtle role in determining the outcome of infection with MTb. Although the *mmpL8::hyg* mutant was not impaired for the initial growth and containment phases of infection in the mouse model, highly significant differences in mouse survival times were observed in experiments performed in two different mice strains. These results suggest a qualitative difference in the nature of the host response that ultimately determines the fate of the infected animal. Similar differences have been observed with recent clinical isolates such as CDC1551 and HN878 (2, 3). The higher levels of cytokines and cytokine receptors expressed in mice infected with the wild-type strain compared with mice infected with the *mmpL8::hyg* mutant are

consistent with a more pronounced suppression of a Th1-type immune response by the wild-type strain than by the *mmpL8::hyg* mutant. The simplest interpretation of this phenotype would be a direct effect of SL-1 on the murine immune system.

For more than 40 years, multiple studies have associated the level of SL-1 produced by specific strains with alterations in virulence in humans and in animal models (15–18, 20, 22, 36). These observational studies of isolates that were far from isogenic stand in contrast to two recent reports that SL-1 mutants in *pks2* were not growth-impaired in either mice or Guinea pigs (23, 24). In one of the mouse studies growth of the isolates was only analyzed for 42 days, while in a second mouse study and in Guinea pigs growth was examined for 100 days. In neither study was survival at the end of infection (typically almost a year later) measured. Our results are entirely consistent with this data and support that the production of SL-1 does not affect the ability of strains to proliferate during the initial replication period, nor does it affect the ability of the host to mount an acquired immune response sufficient to restrict bacterial growth. We have also examined a mutant in *pks2* in such assays. Unfortunately, as we have discovered occurs with many mutants in both *pks* and unrelated loci, this mutant was found to have lost the ability to produce PDIM. Loss of PDIM synthesis appears to be a spontaneous process that occurs in a fraction of mutants generated either by electroporation or by phage-mediated gene replacement strategies. PDIM is an important component of the cell wall structure whose loss has been reported previously to attenuate MTb (10, 42). Thus far the results of long term survival experiments in mice have not been obtained with a PDIM-containing *pks2* mutant, so an exact comparison cannot be made. The possibility also exists that accumulation of SL-N results in an uncharacterized effect on the *mmpL8::hyg* mutant that compromises long term bacterial survival or that MmpL8 transports another unidentified lipid that contributes to virulence. Indeed, Converse *et al.* (23) describe a slight attenuation of their *mmpL8* mutant (but not the corresponding *pks2* mutant) during the bacterial replication and containment phases following high dose intravenous mouse infection but did not assess the relevance of these effects to final survival times of the animals. In contrast to these authors, using the low dose aerosol model we do not see any attenuation of the *mmpL8::hyg* mutant prior to death of the animal. We have also examined as fully as possible the secreted lipid repertoire of the *mmpL8::hyg* mutant and the parental strain without observing any significant differences other than the unique production of SL-N. In any case, the function of SL-1 in human tuberculosis still remains unknown, and more experiments need to be done to clarify the contribution of this lipid to disease outcome in humans.

In summary, we have shown that inactivation of the *mmpL8* gene of MTb interrupts SL-1 synthesis, resulting in accumulation of a precursor to this molecule, SL-N, which we have identified as a family of 2,3-diacyl- $\alpha,\alpha'$ -D-trehalose-2'-sulfates. In the mouse model this alteration results in an apparently normal infection but shows a dramatic effect on ultimate outcome of disease. Since the unique multimethyl-branched fatty acid components of sulfatides (the phthioceranates and hydroxyphthioceranates) are not utilized in any other known molecules, are produced at too low a level to perform a structural function in the cell envelope, and require a significant biosynthetic investment by the cell, it stands to reason that their production likely plays an important role in some aspect of the disease. Studies to explore the importance of the level of sulfatide production with reference to disease outcome in human tuberculosis patients may ultimately lead to stratifying

treatment protocols for such patients and could lead to a further understanding of the dynamic interchange between host and pathogen.

**Acknowledgments**—We thank Dr. C. Guilhot for providing the mycobacterial allelic exchange system; M. Goodwin, J. Gonzales, and S. Freeman for technical assistance; and Dr. Herman Yeh of NIDDK, National Institutes of Health, for performing the NMR.

## REFERENCES

- Daffe, M., and Draper, P. (1998) *Adv. Microb. Physiol.* **39**, 131–203
- Manca, C., Tsenova, L., Barry, C. E., III, Bergtold, A., Freeman, S., Haslett, P. A., Musser, J. M., Freedman, V. H., and Kaplan, G. (1999) *J. Immunol.* **162**, 6740–6746
- Manca, C., Tsenova, L., Bergtold, A., Freeman, S., Tovey, M., Musser, J. M., Barry, C. E., III, Freedman, V. H., and Kaplan, G. (2001) *Proc. Natl. Acad. Sci. U. S. A.* **98**, 5752–5757
- Cole, S. T., Brosch, R., Parkhill, J., Garnier, T., Churcher, C., Harris, D., Gordon, S. V., Eiglmeier, K., Gas, S., Barry, C. E., III, Tekaia, F., Badcock, K., Basham, D., Brown, D., Chillingworth, T., Connor, R., Davies, R., Devlin, K., Feltwell, T., Gentles, S., Hamlin, N., Holroyd, S., Hornsby, T., Jagels, K., Krogh, A., McLean, J., Moule, S., Murphy, L., Oliver, K., Osborne, J., Quail, M. A., Rajandream, M. A., Rogers, J., Rutter, S., Seeger, K., Skelton, J., Squares, R., Squares, S., Sulson, J. E., Taylor, K., Whithead, S., and Barrell, B. G. (1998) *Nature* **393**, 537–544
- Tseng, T. T., Gratwick, K. S., Kollman, J., Park, D., Nies, D. H., Goffeau, A., and Saier, M. H., Jr. (1999) *J. Mol. Microbiol. Biotechnol.* **1**, 107–125
- Bystrykh, L. V., Fernandez-Moreno, M. A., Herrema, J. K., Malpartida, F., Hopwood, D. A., and Dijkhuizen, L. (1996) *J. Bacteriol.* **178**, 2238–2244
- Tekaia, F., Gordon, S. V., Garnier, T., Brosch, R., Barrell, B. G., and Cole, S. T. (1999) *Tuber. Lung Dis.* **79**, 329–342
- Minnikin, D. E., Kremer, L., Dover, L. G., and Besra, G. S. (2002) *Chem. Biol.* **9**, 545–553
- Camacho, L. R., Constant, P., Raynaud, C., Laneelle, M. A., Triccas, J. A., Gicquel, B., Daffe, M., and Guilhot, C. (2001) *J. Biol. Chem.* **276**, 19845–19854
- Cox, J. S., Chen, B., McNeil, M., and Jacobs, W. R., Jr. (1999) *Nature* **402**, 79–83
- Sirakova, T. D., Thirumala, A. K., Dubey, V. S., Sprecher, H., and Kolatukudy, P. E. (2001) *J. Biol. Chem.* **276**, 16833–16839
- Goren, M. B. (1970) *Biochim. Biophys. Acta* **210**, 116–126
- Goren, M. B., Brokl, O., Das, B. C., and Lederer, E. (1971) *Biochemistry* **10**, 72–81
- Goren, M. B., D'Arcy Hart, P., Young, M. R., and Armstrong, J. A. (1976) *Proc. Natl. Acad. Sci. U. S. A.* **73**, 2510–2514
- Goren, M. B., Brokl, O., and Schaefer, W. B. (1974) *Infect. Immun.* **9**, 142–149
- Gangadharam, P. R., Cohn, M. L., and Middlebrook, G. (1963) *Tubercle* **44**, 452–455
- Zhang, L., English, D., and Andersen, B. R. (1991) *J. Immunol.* **146**, 2730–2736
- Zhang, L., Gay, J. C., English, D., and Andersen, B. R. (1994) *J. Biomed. Sci.* **1**, 253–262
- Zhang, L., Goren, M. B., Holzer, T. J., and Andersen, B. R. (1988) *Infect. Immun.* **56**, 2876–2883
- Pabst, M. J., Gross, J. M., Brozna, J. P., and Goren, M. B. (1988) *J. Immunol.* **140**, 634–640
- Brozna, J. P., Horan, M., Rademacher, J. M., Pabst, K. M., and Pabst, M. J. (1991) *Infect. Immun.* **59**, 2542–2548
- Kato, M., and Goren, M. B. (1974) *Infect. Immun.* **10**, 733–741
- Converse, S. E., Mougous, J. D., Leavell, M. D., Leary, J. A., Bertozzi, C. R., and Cox, J. S. (2003) *Proc. Natl. Acad. Sci. U. S. A.* **100**, 6121–6126
- Rousseau, C., Turner, O. C., Rush, E., Bordat, Y., Sirakova, T. D., Kolatukudy, P. E., Ritter, S., Orme, I. M., Gicquel, B., and Jackson, M. (2003) *Infect. Immun.* **71**, 4684–4690
- Pelicic, V., Jackson, M., Reytrat, J. M., Jacobs, W. R., Jr., Gicquel, B., and Guilhot, C. (1997) *Proc. Natl. Acad. Sci. U. S. A.* **94**, 10955–10960
- Sambrook, J., Fritsch, E. F., and Maniatis, T. (1989) *Molecular Cloning: A Laboratory Manual*, 2nd Ed., Cold Spring Harbor Laboratory Press, Cold Spring Harbor, NY
- Domenech, P., Menendez, M. C., and Garcia, M. J. (1994) *FEMS Microbiol. Lett.* **116**, 19–24
- Snapper, S. B., Melton, R. E., Mustafa, S., Kieser, T., and Jacobs, W. R., Jr. (1990) *Mol. Microbiol.* **4**, 1911–1919
- Folch, J., Lees, M., and Sloane Stanley, G. H. (1957) *J. Biol. Chem.* **226**, 497–509
- Slayden, R. A., and Barry, C. E., III (2001) in *Mycobacterium tuberculosis Protocols* (Parish, T., and Stoker, N. G., eds) Vol. 54, pp. 229–245, Humana Press Inc., Totowa, NJ
- Constant, P., Perez, E., Malaga, W., Laneelle, M. A., Saurel, O., Daffe, M., and Guilhot, C. (2002) *J. Biol. Chem.* **277**, 38148–38158
- Soto, C. Y., Andreu, N., Gibert, I., and Luquin, M. (2002) *J. Clin. Microbiol.* **40**, 3021–3024
- Kaplan, E. L., and Meier, P. (1958) *J. Am. Stat. Assoc.* **53**, 457–481
- Morse, W. C., Dail, M. C., and Olitzky, I. (1953) *Am. J. Public Health* **43**, 36–39
- Hughes, D. E., Moss, E. S., Hood, M., and Henson, M. (1954) *Am. J. Clin. Pathol.* **24**, 621–625
- Middlebrook, G., Coleman, C. M., and Schaefer, W. B. (1959) *Proc. Natl. Acad. Sci. U. S. A.* **45**, 1801–1804
- Mougous, J. D., Leavell, M. D., Senaratne, R. H., Leigh, C. D., Williams, S. J., Riley, L. W., Leary, J. A., and Bertozzi, C. R. (2002) *Proc. Natl. Acad. Sci. U. S. A.* **99**, 17037–17042
- Alugupalli, S., Laneelle, M. A., Larsson, L., and Daffe, M. (1995) *J. Bacteriol.* **177**, 4566–4570
- Baer, H. H. (1993) *Carbohydr. Res.* **240**, 1–22
- Goren, M. B., Brokl, O., and Das, B. C. (1976) *Biochemistry* **15**, 2728–2735
- Belisle, J. T., Vissa, V. D., Sievert, T., Takayama, K., Brennan, P. J., and Besra, G. S. (1997) *Science* **276**, 1420–1422
- Camacho, L. R., Ensergueix, D., Perez, E., Gicquel, B., and Guilhot, C. (1999) *Mol. Microbiol.* **34**, 257–267